Journal of *Marine Science and Engineering*

MDPI

Article

The Impact of Pre-Existing Faults on Fault Geometry during Multiphase Rifts: The Jiyang Depression, Eastern China

Di Wang [1,*], Linlong Yang [2], Wei Li [3] and Xidong Wang [1]

[1] School of Geology and Mining Engineering, Xinjiang University, Urumqi 830046, China; microdifficult@xju.edu.cn
[2] Working Station for Postdoctoral Scientific Research, Shengli Oilfield, Dongying 257001, China; t-yanglinlong.slyt@sinopec.com
[3] School of Geosciences, China University of Petroleum, Qingdao 266580, China; 20070017@upc.edu.cn
* Correspondence: wangdi@xju.edu.cn

Abstract: The combination of multi-phase extension and pre-existing fault reactivation results in a complex fault pattern within hydrocarbon-bearing basins, affecting hydrocarbon exploration at different stages. We used high-resolution 3D seismic data and well data to reveal the impact of multi-phase extension and pre-existing fault reactivation on Cenozoic fault pattern changes over time in the Jiyang Depression of eastern China. The results show that during the Paleocene, a portion of NW-striking pre-existing faults reactivated under NS extension and controlled the basin structure (type 1). Other parts of the NW-striking pre-existing faults stopped activity and served as weak surfaces, and a series of NNE-striking faults were distributed in an en-echelon pattern along the NW direction at shallow depths (type 2). In areas unaffected by pre-existing faults, NE-striking faults formed perpendicular to regional stresses. During the Eocene, the regional stresses shifted clockwise to near-NS extension, and many EW-striking faults developed within the basin. The NE-striking faults and the EW-striking faults were hard-linked, forming the ENE-striking curved faults that controlled the structure in the basin (type 3). The NNE-striking faults were distinctly strike-slip at this time, with the ENE-striking faults forming a horsetail pattern at their tails. Many ENE-striking faults perpendicular to the extension direction were formed in areas where the basement was more stable and pre-existing faults were not developed (type 4). There were also developing NS-striking faults that were small in scale and appeared in positions overlapping different main faults (type 5). Additionally, different fault patterns can guide different phases of hydrocarbon exploration. Type 1, type 2, and type 3 faults are particularly suitable for early-stage exploration. In contrast, type 4 and type 5 faults are more appropriate for mature exploration areas, where they may reveal smaller hydrocarbon reservoirs.

Keywords: non-coaxial extension; fault reactivation; fault pattern; Jiyang depression

Citation: Wang, D.; Yang, L.; Li, W.; Wang, X. The Impact of Pre-Existing Faults on Fault Geometry during Multiphase Rifts: The Jiyang Depression, Eastern China. *J. Mar. Sci. Eng.* **2023**, *11*, 1971. https://doi.org/10.3390/jmse11101971

Academic Editor: Dimitris Sakellariou

Received: 4 September 2023
Revised: 3 October 2023
Accepted: 10 October 2023
Published: 12 October 2023

1. Introduction

In nature, most rift basins have experienced multiple phases of tectonic activity from the Paleozoic to the Cenozoic, resulting in many non-coaxial extension rift phases [1,2]. Additionally, these activities have further influenced the diverse behaviors of pre-existing faults. The combination of multi-phase extension and pre-existing fault activity has impacted the growth and development process of fault networks, leading to the formation of intricate fault systems consisting of faults oriented in different directions [3–6]. Notable examples of such basins include eastern China (the Bohai Bay Basin (BBB) [7–9]; the South China Sea (SCS) [10–12]); the North Sea rift [13–15]; the Thailand Basin [16,17]; and the North West Shelf, Australia [18,19]. These regions experience multi-phase stress, causing the pre-existing faults to reactivate in later tectonic events [20]. Furthermore, basins are frequently separated by pre-existing faults, resulting in changes to the basin architecture.

Concurrently, newly formed basins tend to exhibit fault networks composed of faults with different ages, strikes, and properties [5,21,22]. Consequently, fault networks in rift basins are often comprised of non-colinear faults [23–25], leading to complex fault patterns [9,26]. These different types of fault patterns affect the process of sediment entering the basin, further affecting the characteristics of sedimentary facies distribution, and ultimately leading to differences in oil and gas distribution [2,27,28].

The Jiyang Depression, located In eastern China, stretches in a NEE direction and covers an area of approximately 29,000 square kilometers (Figure 1). The eastern part of the depression is bounded by the Tan–Lu Fault Zone, while the western and northern parts are adjacent to the Chengning Uplift. The southern part, on the other hand, is surrounded by the Qi–Guang Fault and Luxi Uplift [6,8]. Due to the subduction of the Pacific plate, Indo-Chinese plate collisions, and large-scale faulting [29,30], it is recognized as one of the most seismically active regions on Earth. These tectonic processes occurred either simultaneously or at different times, resulting in varying stress regimes during the Cenozoic era in eastern China. Within the basin, extensional, strike-slip, and inversion structural styles can be observed, albeit with spatial differences [31,32]. Initially, it was believed that the fault characteristics in Cenozoic basins in eastern China were caused solely by simple extensional stress. However, subsequent studies revealed that pre-existing structures (such as faults, basement structures, and salt structures) within rift basins significantly impact fault characteristics [33,34]. Additionally, multi-phase extension leads to localized stress rotation and complex fault characteristics [14,20].

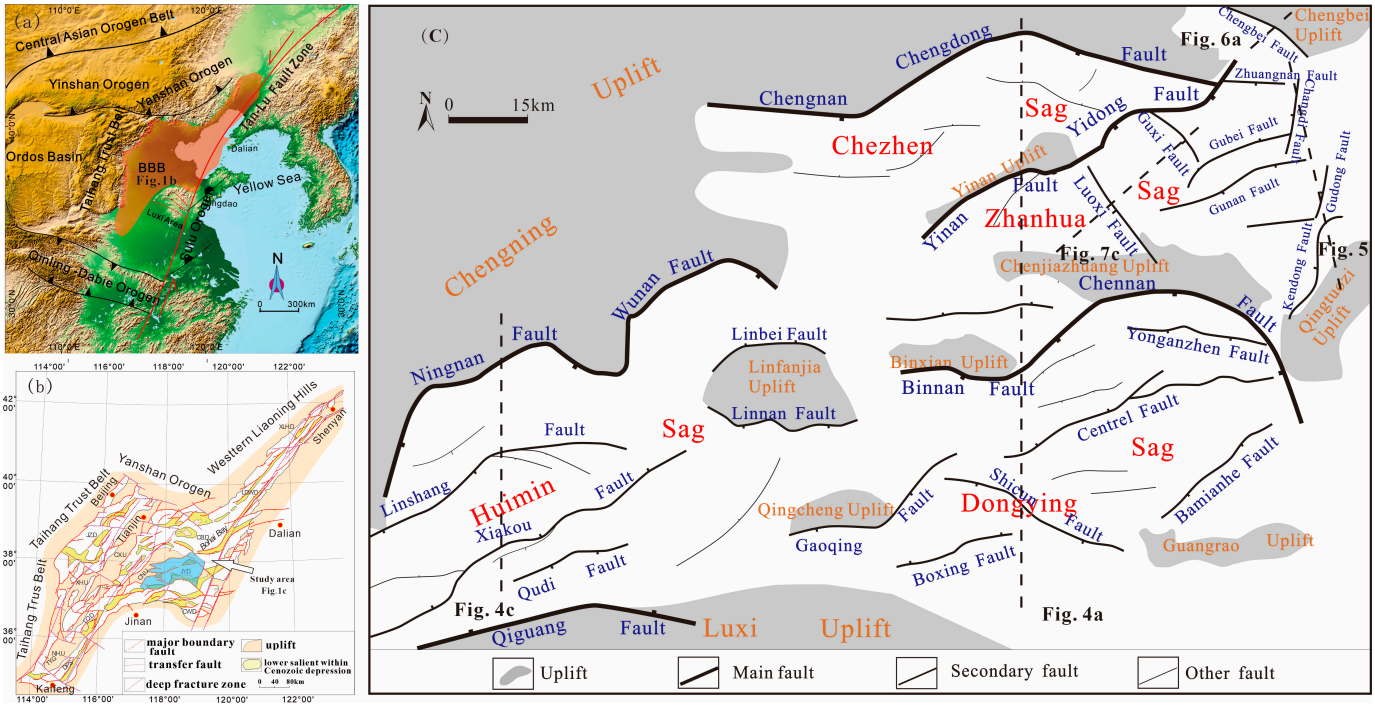

Figure 1. (**a**) Bohai Bay Basin (BBB) is located in northern China. (**b**) Tectonic map of the Bohai Bay Basin and the research area (Jiyang Depression). (**c**) The fault system illustrates the structural framework of the Jiyang Depression.

In this study, we analyze the fault patterns and basin evolution using high-resolution 3D seismic data and well-logging data from the Shengli Oil Field, which has been subjected to extensive hydrocarbon exploration within the Jiyang Depression. The availability of abundant seismic data provides us with a unique opportunity to examine local stress conditions in the study area and compare them with regional stress conditions in the Bohai Bay Basin. Through this analysis, we aim to explore the influence of both regional and local stress on tectonic evolution. By studying the fault characteristics and evolutionary

process specific to the study area, we seek to elucidate the development patterns of the faults and identify the controlling factors responsible for the spatial variability in fault evolution within rift basins. As the Jiyang Depression represents a crucial hydrocarbon area in eastern China, comprehending the spatial variability of fault patterns holds immense importance for effective hydrocarbon exploration.

2. Geological Setting

2.1. Bohai Bay Basin (BBB)

The Cenozoic BBB is a rift basin located in the northern region of eastern China, with an overall area of approximately 200,000 km^2. The basin's dynamics are influenced by the Pacific plate and the Tan–Lu strike-slip fault zone. Over time, the basin has undergone various tectonic processes such as compression, extension, and strike-slip, forming multiple-stage faults with different orientations and characteristics [35,36].

During the Triassic to Early Jurassic epochs, the collision between the North and South China Blocks occurred within the Qinling–Dabie orogenic belt, resulting in the development of numerous NW-striking thrust faults and folds within the BBB [8,37,38]. In the Middle to Late Jurassic, the basin experienced weak compression, leading to the deposition of thicker sedimentary layers. In the Cretaceous epoch, magma upwelling caused significant changes in the dynamics of the BBB [39,40]. The paleo-Pacific plate moved in a north-northwest direction, with a subduction rate of 300 mm/a, causing the basin dynamics to shift from compression to extension [8,29]. As a result, the NW-striking faults underwent negative inversion and transformed into normal faults [41].

In the early Cenozoic era, the BBB inherited the dynamic background established during the Cretaceous epoch, with NW-striking faults controlling the overall structure of the basin [35,42]. Around 43 million years ago, during the Eocene epoch, the subduction direction of the Pacific plate changed from NNW to WNW and continued throughout the Paleocene epoch [41,43,44]. This subduction occurred at a high angle of approximately 80°, leading to a predominantly north–south-oriented extensional background in eastern China. Notably, the Tan–Lu Fault zone underwent a change in rotation from right to left during this period [20,45]. Consequently, the BBB experienced a combination of extensional and strike-slip stresses, forming the NW-, NNE-, ENE-, and EW-striking faults within the basin. This complex fault pattern contributes to the diverse structural characteristics observed within the basin.

2.2. Jiyang Depression

The Jiyang Depression is a significant geological unit in the southwestern region of the Bohai Bay Basin (BBB) in eastern China. It stretches in an ENE direction and is known for its abundant petroleum resources. The depression is bordered by the Chengning Uplift to the north, the Luxi Uplift to the south, the Tan–Lu strike-slip fault to the east, and the Linqing Depression to the west [8]. It is a rift basin formed on the Paleozoic basement of northern China during the Cenozoic era. The region has experienced various tectonic events including the Indo-Chinese (290–210 Ma), Yanshan (210–65 Ma), and Himalayan movements (65 Ma–now), resulting in the development of complex fault patterns [2,20].

Within the study area, four sags can be identified: the Chezhen Sag, Zhanhua Sag, Huimin Sag, and Dongying Sag. Initially, researchers identified numerous NE-striking faults in the Cenozoic basin [7,8]. Benefiting from extensive petroleum exploration, several NW-striking reverse faults in the Mesozoic basin were subsequently revealed. These NW-striking faults cut through the basement and experienced extensional or transtensional stresses during the Cenozoic era, leading to negative inversion processes [7,20,33]. These faults played a crucial role in shaping the late Mesozoic and early Cenozoic basins. The orientation of these faults provides valuable information about the seismic profile, allowing for the study of multi-phase stresses and pre-existing faults on the basin structure and fault pattern.

The Jiyang Depression is a superimposed basin with deposits from the Mesozoic to Cenozoic epochs, developed on the North China Craton. Figure 2 illustrates the stratigraphy of the study area from bottom to top. The Cambrian–Ordovician epoch is dominated by shallow marine carbonate strata. The Carboniferous–Permian epoch is characterized by interfacial and fluvial clastic phases. The Jurassic and Early Cretaceous epochs feature coal-bearing clastic rocks, red clastic rocks, and locally developed volcanic rocks. The Paleocene stratum of the Paleogene era has limited exposure. The Eocene–Oligocene strata consist mainly of lacustrine clastic rock. The Neogene–Quaternary epoch is characterized by fluvial facies clastic rock.

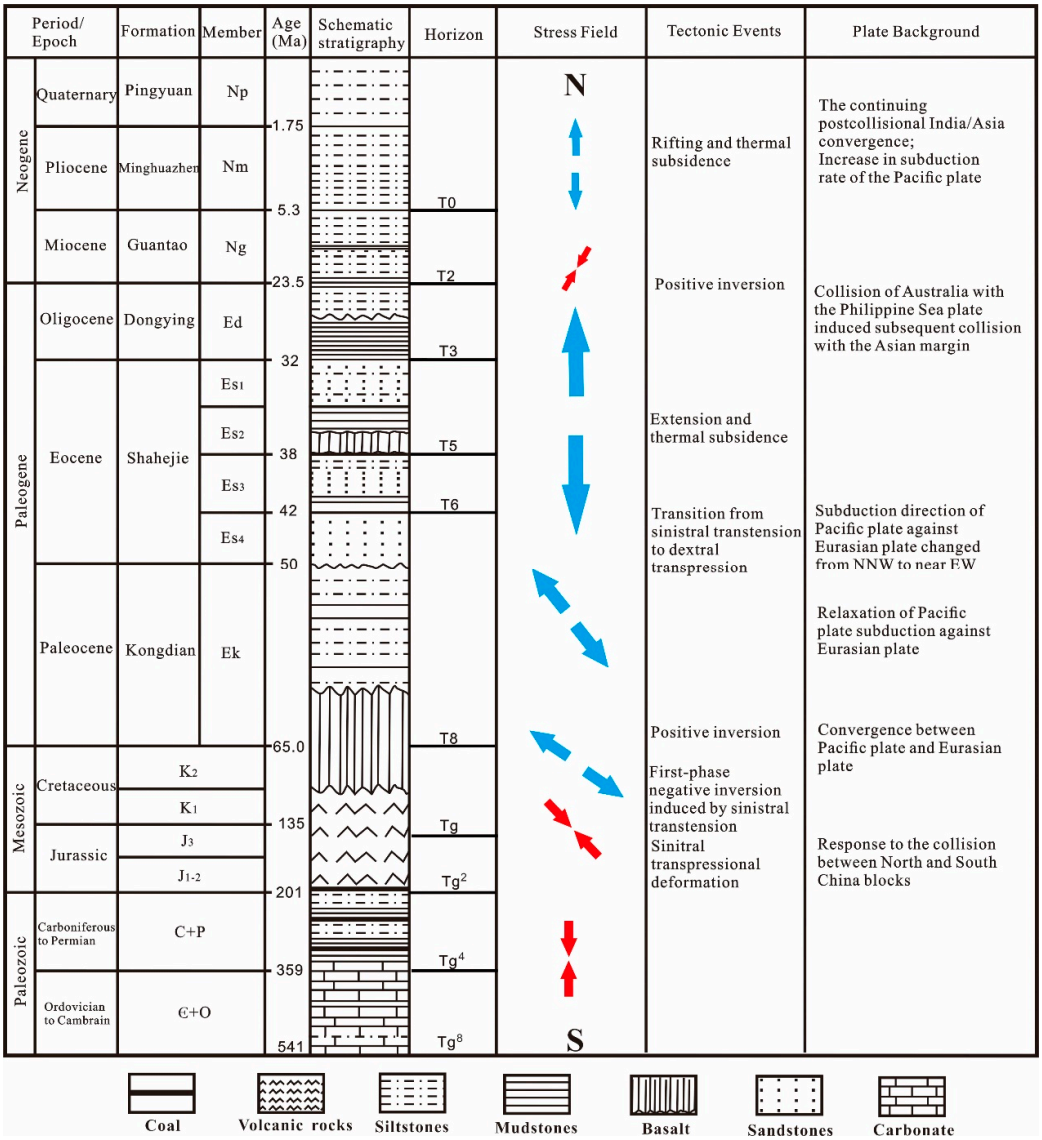

Figure 2. The simple stratigraphic column in the Jiyang Depression. The stratigraphic column indicates the main seismic horizons and stratigraphic units in the research area. Mainly relying on biostratigraphy and well report data from an oil company, it roughly describes the age of the stratigraphic ages (Wang et al., 2022) [20].

The Cenozoic strata include the Paleogene and Neogene strata. The Paleogene strata include the Kongdian Formation, Shajie Formation, and Dongying Formation from bottom to top, while the Neogene strata include the Guantao Formation, Pingyuan Formation, and Minghuazhen Formation from bottom to top. Unconformities resulting from tectonic events led to the division of the entire sedimentary sequence into several structural layers.

These structural layers are reflected onto the seismic reflection interface, marked by Tg^8, Tg^4, Tg^2, Tg, T8, T6, T5, T3, T2, and T0 in the article (Figure 2).

Similar to other regions in eastern China, the tectonic evolution of the Jiyang Depression involved a stable development stage during the Paleozoic era, followed by activation and rift basin development in the Mesozoic and Cenozoic eras.

3. Materials and Methods

This study focused on analyzing seismic reflection data, both in 2D and 3D, collected by the Shengli Oil Branch Company of Sinopec Corp (China Petroleum & Chemical Corporation, Dongying, China) in the Jiyang Depression. The 3D seismic data consist of 9 separate seismic cubes covering the main hydrocarbon areas of the region (Figure 3), with a line spacing of 25 m and a depth range of up to 5 s of two-way travel time (TWT). These seismic data primarily exhibit Cenozoic sedimentary characteristics, but also include some Mesozoic sedimentary features. The study area is further complemented by nearly 500 2D seismic lines that cover different sags and traverse in the NNE–SSW, EW, and NS directions. Moreover, over 100 well data points were collected, providing additional information that allows for accurate seismic interpretation of sedimentary layers and faults. Most wells in the area penetrate the Cenozoic strata, while only a few reach the Paleozoic strata.

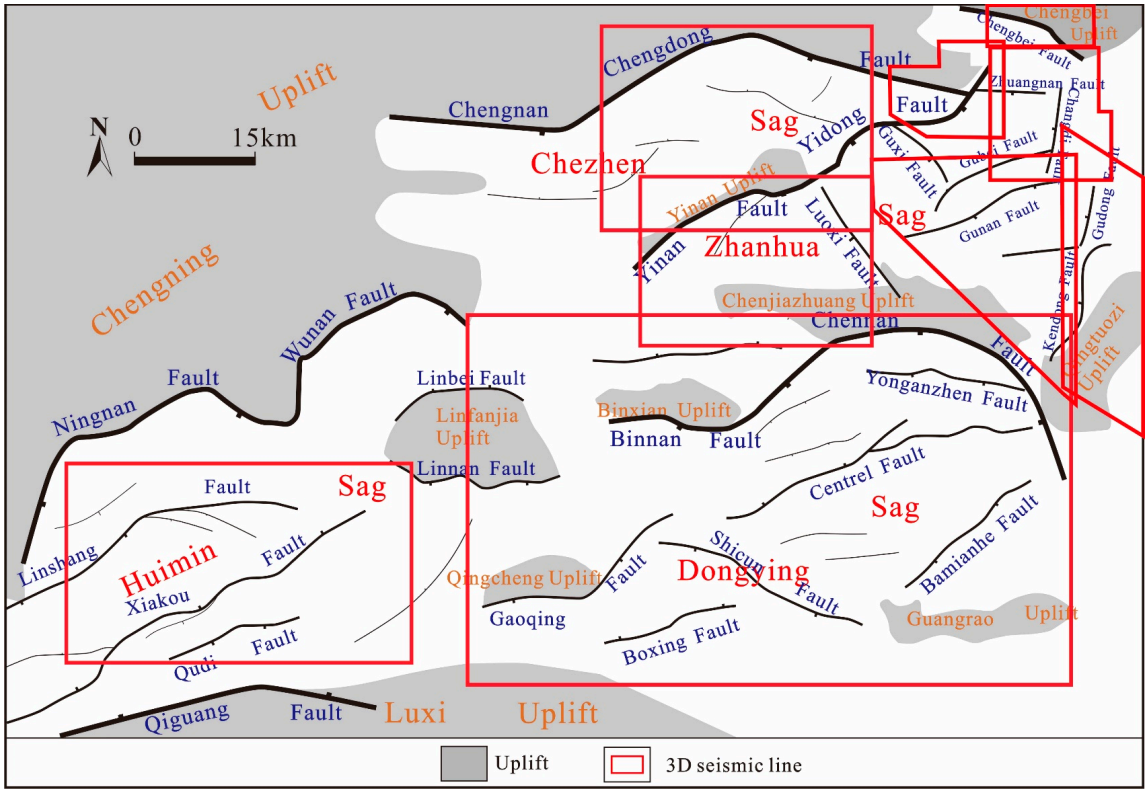

Figure 3. The seismic data used in the research area. Includes 9 seismic cubes.

By processing the seismic data volume, different time slices were obtained, combined with the ant tracking method, and shallow wells that were drilled in the study area were used. Six key Cenozoic stratigraphic horizons (T8, T6, T5, T3, T2, and T0) were interpreted. The activity rates of major faults with different orientations were calculated to understand the structural history of the region. Through Petrel software 2018, the data volume was finely interpreted and combined with the time slice, which was used to draw the structural maps of key layers (Es_3, Ed). Based on the evolutionary characteristics of the study area, different types of fault pattern maps were created to assess the impact of multi-stage extension and reactivation of pre-existing faults on fault geometry.

4. Fault Geometries of the Jiyang Depression

4.1. NE-Striking Faults

During the Cenozoic era, a significant number of NE-striking faults emerged in the Jiyang Depression, establishing the primary fault network system. Major half-graben basins within the region are bounded by several large-scale boundary faults, including the Ningnan–Wuannan Fault, Qi–Guang Fault, Yidong–Yinan Fault, and Chenan Fault, which developed on a large scale and are >100 km in length. These faults contribute to the displacement of the basement across them and exhibit a "zigzag" pattern in map view, characterized by alternating NE- and ENE-striking segments. The structural features of the Jiyang Depression are greatly influenced by these faults.

Moreover, numerous NE-striking faults developed within the basin, governing the characteristics of secondary structural units such as sags and uplifts. For instance, the Huimin Sag is influenced by the Xiakou Fault and Linshang Fault, while the Dongying Sag is affected by the Central Fault, and the Zhanhua Sag is impacted by the Gubei Fault. Furthermore, the sags contain additional NE-striking faults that shape the development of local fault blocks (see Figure 4).

Vertically, in terms of fault geometry, the entire fault plane demonstrates a steep upper part, transitioning into a listric shape at lower depths. These boundary faults intersect multiple layers, extending from the basement to the Neogene strata. They combine with secondary faults to form a Y-shaped geometry. In the sags, smaller-scale faults with ENE- to EW-striking orientations are primarily observed in shallow layers, specifically in the Eocene and Oligocene strata (Figure 4).

Within the Linnan area located in the southwest part of the Jiyang Depression, deep-seated NE-striking faults exhibit steep dips. When viewed in plan view, the secondary faults with an ENE-striking orientation form a horsetail structure alongside the main NE-striking fault, indicating transtensional characteristics. This phenomenon primarily arises from strike-slip activity along the Lanliao Fault in the western region and regional stress changes [9]. In other regions of the Jiyang Depression, the ENE-striking faults display normal fault characteristics, aligning with the NNW–SSE extension pattern observed throughout eastern China during the Cenozoic era [8].

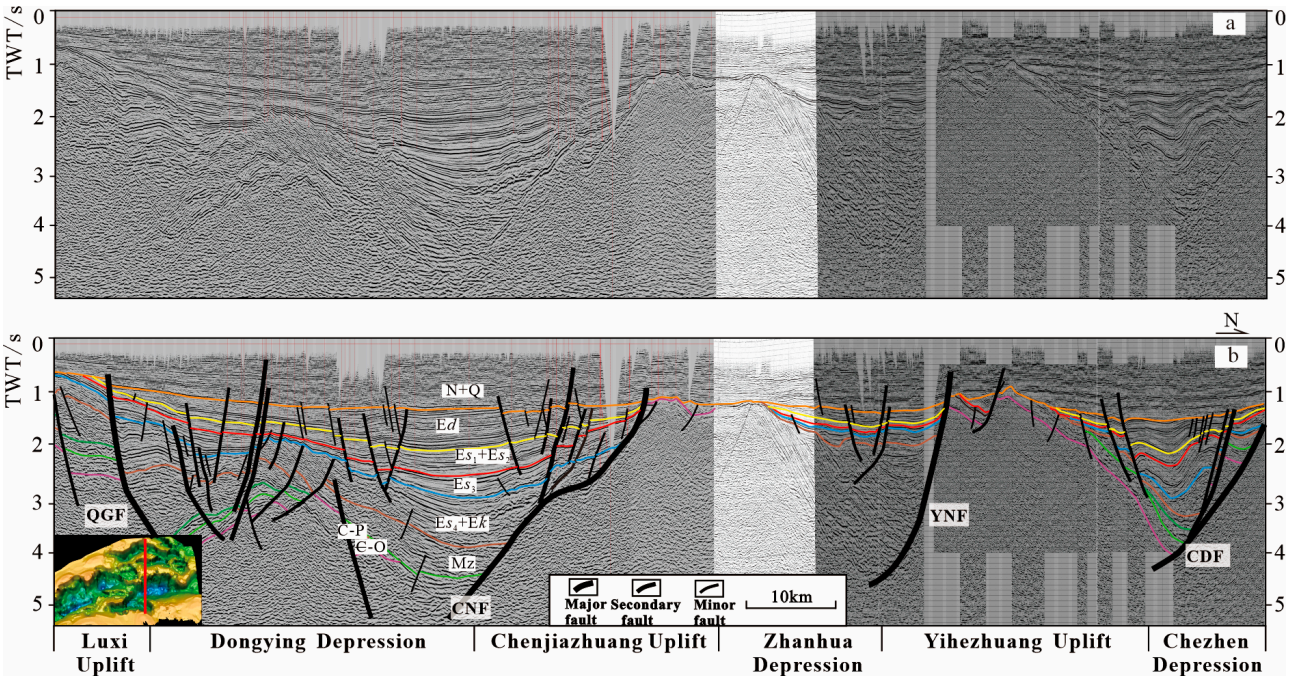

Figure 4. *Cont.*

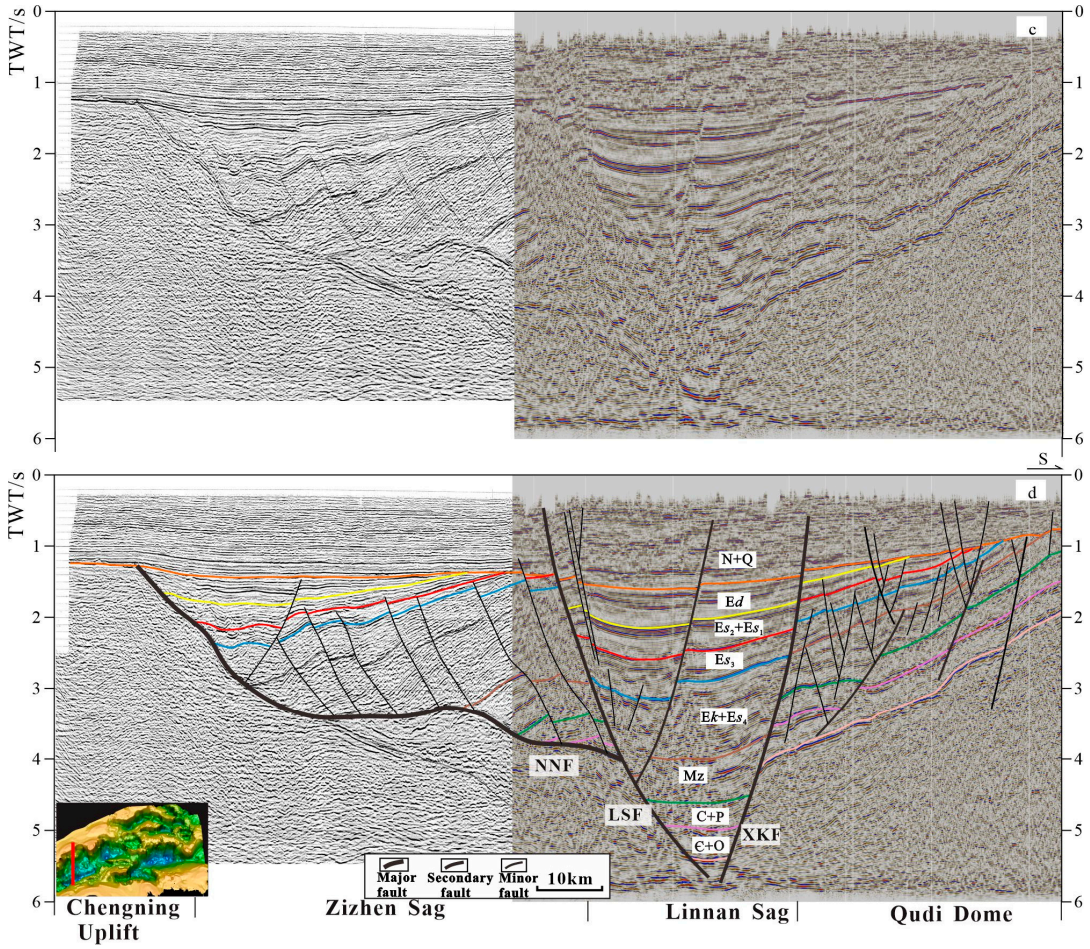

Figure 4. The SN-striking seismic profile reflects the characteristics of the NEE-striking fault. The location is indicated in Figure 1c and shown in plan view. Seismic profiles (**a**,**b**) show the typical feature of the ENE-striking fault in the eastern part of the study area. Abbreviations: CNF, Chennan Fault; YNF, Yinan Fault; CDF, Chengdong Fault. Seismic profiles (**c**,**d**) show the typical features of the NEE-striking fault in the western part of the study area. Abbreviations: NNF, Ningnan Fault; LSF, Linshang Fault; XKF, Xiakou Fault. The boundary faults are listric normal faults and cut the Paleozoic strata. The ENE-striking fault controls the structural characteristics of the study area.

4.2. NNE-Striking Faults

The eastern part of the Jiyang Depression primarily exhibits a concentration of NNE-striking faults, in contrast to the relatively underdeveloped western region. Notably, the area contains several representative faults, namely the Changdi Fault, Gudong Fault, and Kendong Fault, which are specifically developed in the Changdi–Kendong area (see Figure 1c). A deep-level analysis using seismic time slices reveals the clear and continuous nature of the NNE-striking faults; these NNE-striking faults are combined in an en-echelon style and extend along the NW direction. Conversely, at shallower depths, these NNE-striking faults display discontinuities and develop numerous NE-striking secondary faults, distributed in an en-echelon pattern along the NNE direction (refer to Figure 5a,b). Vertically, these fault planes exhibit steep dips, extending from the basement upward and reaching up to the Oligocene strata. They form a flower-shaped geometry when combined with secondary faults within the Cenozoic strata (Figure 5c,d). These NW-striking faults distinctly exhibit strike-slip characteristics, which are closely associated with the strong strike-slip effect observed along the adjacent Tan–Lu fault zone [20].

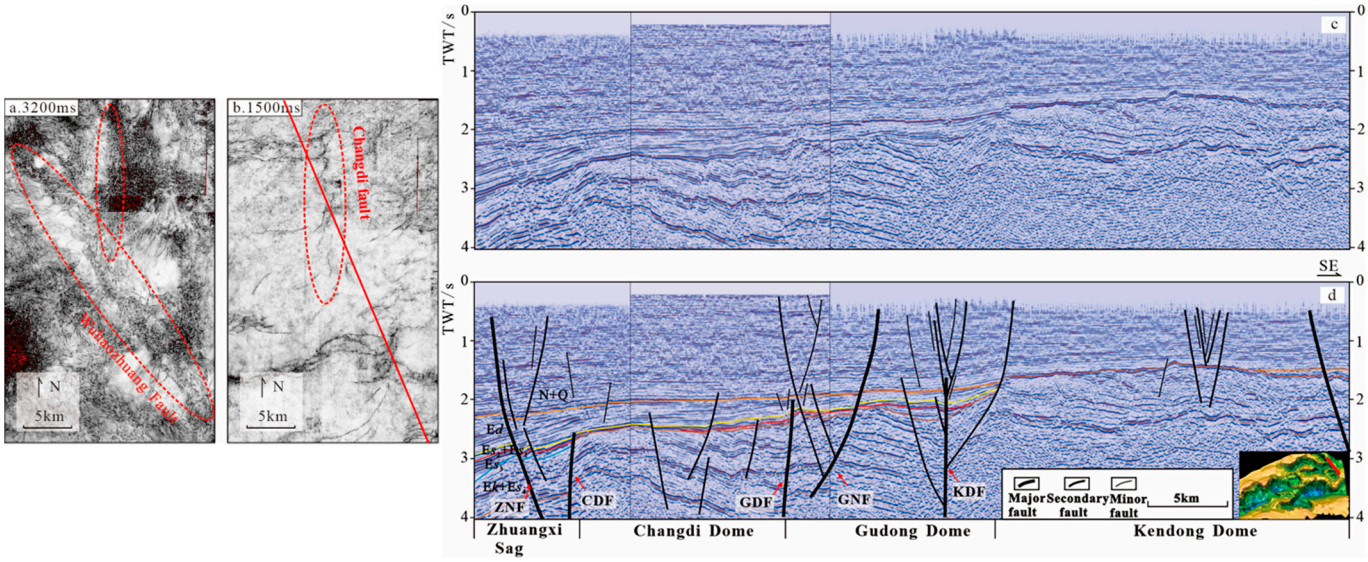

Figure 5. The NW-striking seismic profile reflects the characteristics of the NNE-striking fault. The location is indicated in Figure 1c and (**d**). (**a**) NNE-and NW-striking faults are mainly large-scale boundary faults and continue at greater depths. (**b**) NNE-striking faults are discontinued and NE-striking faults distributed in an en-echelon pattern. (**c**,**d**) NNE-striking faults are approximately upright and form flower-shaped structures with shallow secondary faults. Abbreviations: ZNF, Zhuangnan Fault; CDF, Changdi Fault; GDF, Gudong Fault; GNF, Gunan Fault; KDF, Kendong Fault.

4.3. NW-Striking Faults

The NW-striking fault is the main fault in the Mesozoic strata in the Jiyang Depression, which is processed from negative structural inversion resulting from late Triassic thrust to Cretaceous normal faults [7,8]. During the Paleogene, the fault activity weakened and became a transfer zone for the development of the Cenozoic fault system. The seismic time slice reveals that these faults are continuous at deep levels (Figures 6 and 7). However, at the shallow level, there is no NW-striking fault visible in the west (Figure 7), while in the east, the NW-striking fault is still visible, and it is abutted by the ENE-striking faults (Figure 6). Vertically, the dip angle is relatively gentle, with some faults extending upward to the base of the Eocene strata, and others extending upward to the Neogene strata. The stratigraphic distribution is thick in the west and thin in the east from the Paleozoic to the Lower and Middle Jurassic. The stratigraphic distribution of the late Jurassic and Cretaceous epoch is wedge-shaped, gradually thickening from west to east. During the Cenozoic era, the strata that developed inherited the wedge-shaped structure of the Upper Mesozoic strata. The western part is thin, and the eastern part is thick. The Neogene and Quaternary strata fill the depression and tend to be flat (Figures 6 and 7).

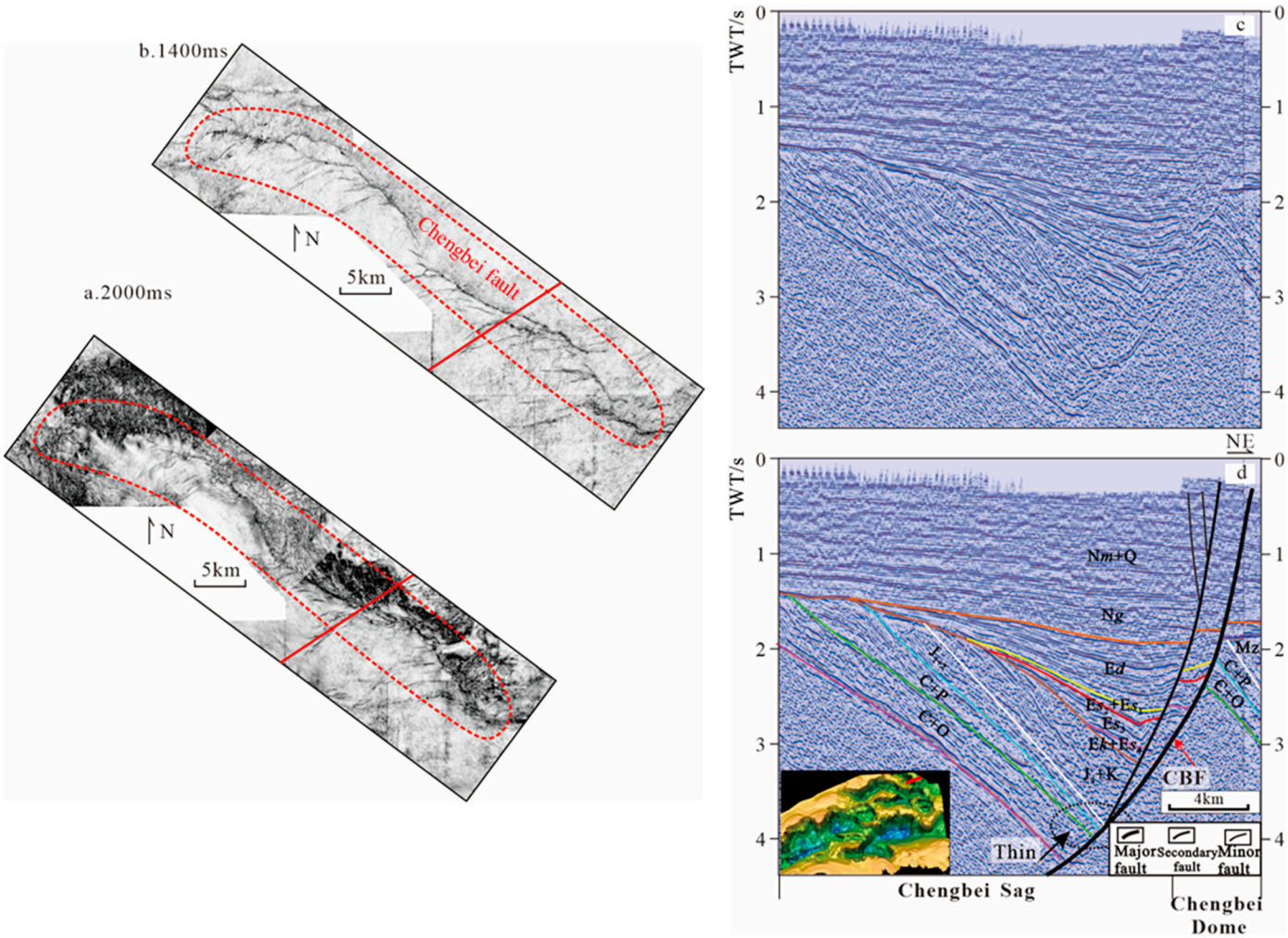

Figure 6. The NE-striking seismic profile reflects the characteristics of the NW-striking fault. The location is indicated in Figure 1c and (**a**,**b**). (**a**) NW-striking faults are mainly large-scale boundary faults and continue at greater depths. (**b**) NE- and ENE-striking secondary faults abut the NW-striking fault. (**c**,**d**) NW-striking faults cut across the Cenozoic and Paleozoic layers, suggesting their continuous activity. This stratigraphic distribution is thick in the west and thin in the east from the Paleozoic to the Lower and Middle Jurassic. The upper Jurassic and Cretaceous strata are exactly the opposite, with a wedge-shape that is thin in the west and thick in the east. This indicates that the NW-striking faults reversed in the Mesozoic. Abbreviation: CBF, Chengbei Fault.

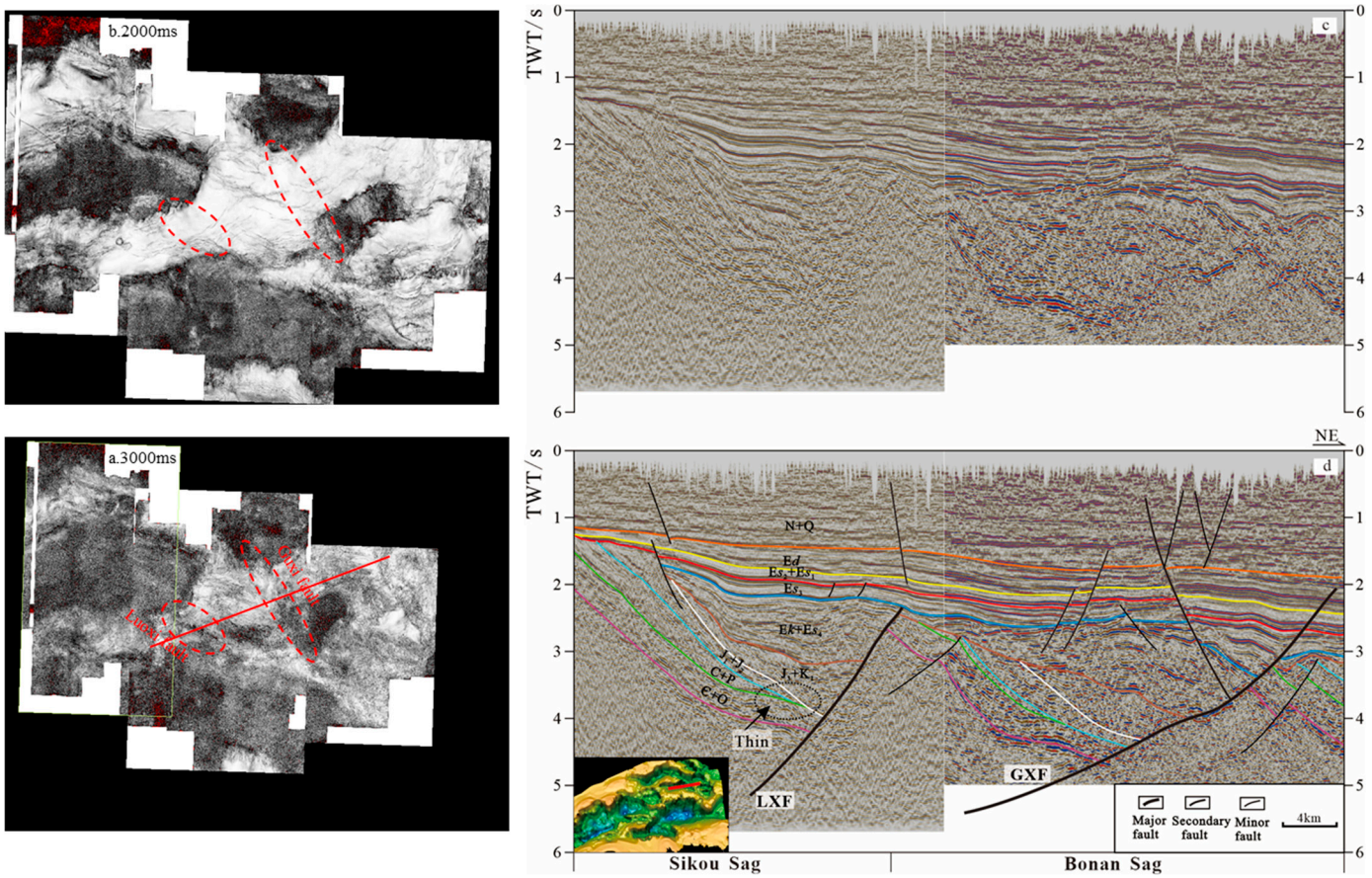

Figure 7. The NE-striking seismic profile reflects the characteristics of the NW-striking fault (Luoxi fault, Guxi fault). The location is indicated in Figure 1c and (**a**). (**a**) NW-striking faults are mainly large-scale boundary faults and continue at greater depths. (**b**) ENE-striking faults become the main faults. (**c**,**d**) Luoxi Fault only cuts across the Mesozoic and Paleozoic layers, suggesting it stopped activities in the Cenozoic. The Guxi Fault cuts across the Cenozoic and Paleozoic layers. Abbreviations: LXF, Luoxi Fault; GXF, Guxi Fault.

4.4. ENE(-Near EW)-Striking Faults

The ENE-striking faults developed on a small scale, and the development time was relatively late. In the plan view, they are mainly distributed in parallel. Appearing at the tips of the main faults, the main faults combine to form a horsetail (Figures 5 and 6). The EW-striking faults are the most developed in the central basin, especially in shallow layers.

4.5. NS-Striking Faults

The NS-striking faults developed on a small scale. In the plan view, they extend for a short distance; vertically, they only cut one layer or develop within the same layer. The NS-striking faults always occur in the fault blocks, especially in the overlapping positions of different main faults, making the fault network complex (Figure 8).

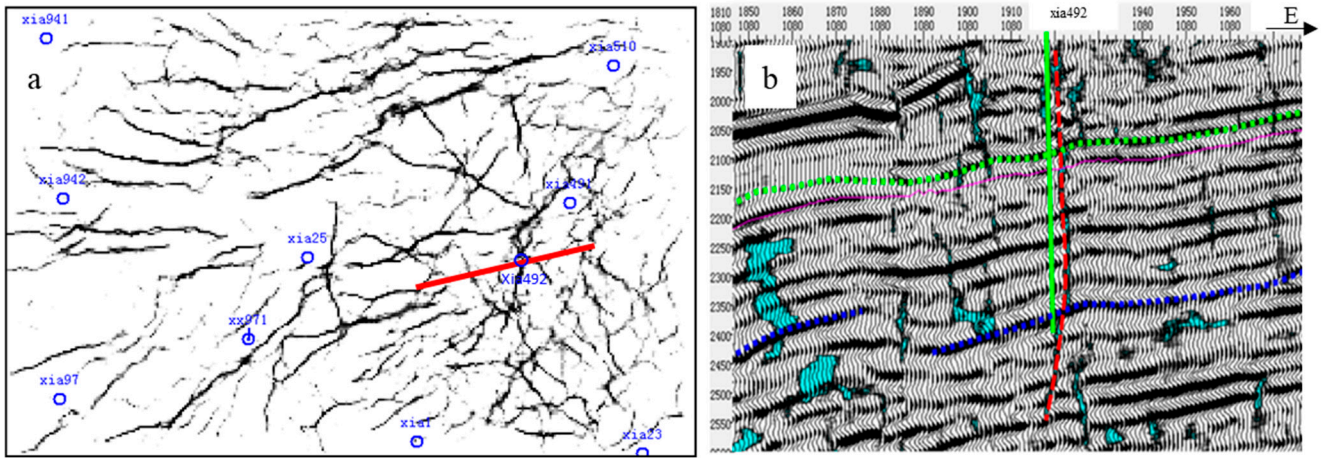

Figure 8. The ENE-striking seismic profile reflects the characteristics of the NS-striking fault. The location is indicated in Figure 7a. (**a**) shows the local coherent slices, which can identify small faults that are difficult to explain. (**b**) uses ant body tracking, and small faults in the NS-striking direction can be seen.

Overall, the Cenozoic fault network in the Jiyang Depression is composed of multi-directional faults with multiple properties. The NE-striking normal faults form the main framework of the fault system, reflecting regional NNW–SSE extension. Affected by the Tan–Lu Fault zone, a large number of NNE-striking faults have developed in the eastern part of the study area, exhibiting obvious strike-slip characteristics. The NW-striking faults are the basement faults of the Cenozoic basin, which underwent a structural inversion process in the Mesozoic era. The Cenozoic strata developed in the northeastern region, reflecting the oblique extension effect. The NS-striking faults are mostly small faults that played a role in the transformation.

5. Kinematic Analysis

5.1. Fault Activity in the Jiyang Depression

Figure 9 shows changes in fault activity across different fault strikes in the study area: (1) the ENE-striking boundary faults of the Jiyang depression started to activate during Mesozoic and have remained active until present. Their peak activity was observed during the Es_3 sub-sequence, which occurred during the Paleocene. ENE-striking faults had the strongest activity during this period and played a significant role in controlling the sedimentary characteristics of various secondary structural units in the Jiyang Depression. An example is the Xiakou Fault in the Huimin Sag. (2) The NNE-striking faults show both dip-slip and strike-slip movements. Their activity rate was strongest during the Es_3 sub-sequence and gradually weakened over time. Examples of NNE-striking faults include the Kendong Fault and Changdi Fault (Figure 9). (3) The NW-striking faults were active earlier and controlled the development of Mesozoic–Paleozoic strata. From the seismic profile, it is clear that negative inversion occurred during the Late Jurassic–Cretaceous and the nature of faults changed from thrust faults to normal faults (Figures 6 and 7). During the Cenozoic, some NW-striking faults activity rates reached their peak during the Es_3 sub-sequence, and then gradually weakened until the Neogene (such as the Chengbei Fault and Guxi Fault). Some NW-striking faults stopped activity in the Es_3 sub-sequence (such as the Wuhaozhuang Fault and Luoxi Fault) [20]. (4) The NS-striking faults are small normal faults with weak activity (Figures 7 and 8).

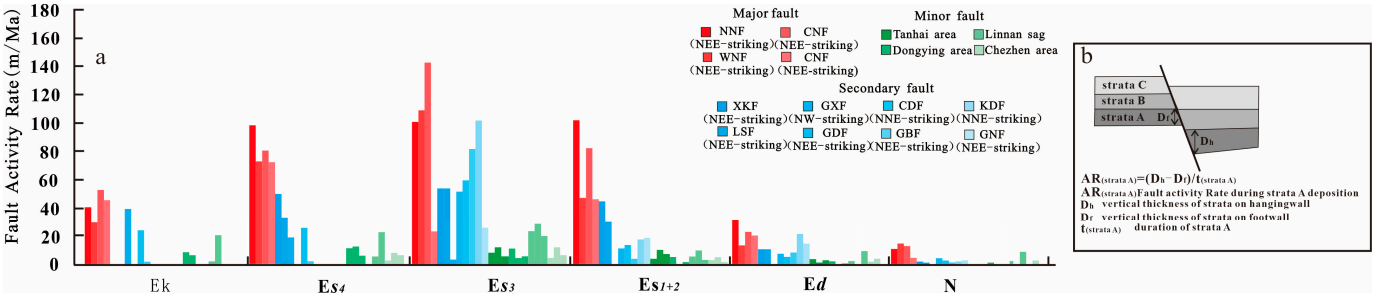

Figure 9. (**a**) The fault activity rate (fault activity) of the different faults during different periods in the study area shows the intensity of fault activity. (**b**) Measurement of the activity rate of dip-slip faulting. Abbreviations: NNF, Ningnan Fault; CNF, Chengnan Fault; WNF, Wunan Fault; CNF, Chengnan Fault; XKF, Xiakou Fault; GXF, Guxi Fault; CDF, Changdi Fault; KDF, Kendong Fault; LSF, Linshang Fault; GDF, Gudong Fault; GBF, Gubei Fault; GNF, Gunan Fault.

5.2. Jiyang Depression Fault Pattern Change with Time

The fault pattern in the Jiyang Depression changed over time (Figure 10). The two phases of extension occurred during the Paleocene and Eocene [8,41,46]. During the second extension, some NW-striking faults reactivated and formed new faults. Cenozoic basins exhibit various fault patterns, including curved faults, horsetail structures, and en-echelon patterns. Under the influence of multi-phase extension and pre-existing faults, most of these fault patterns evolved over time.

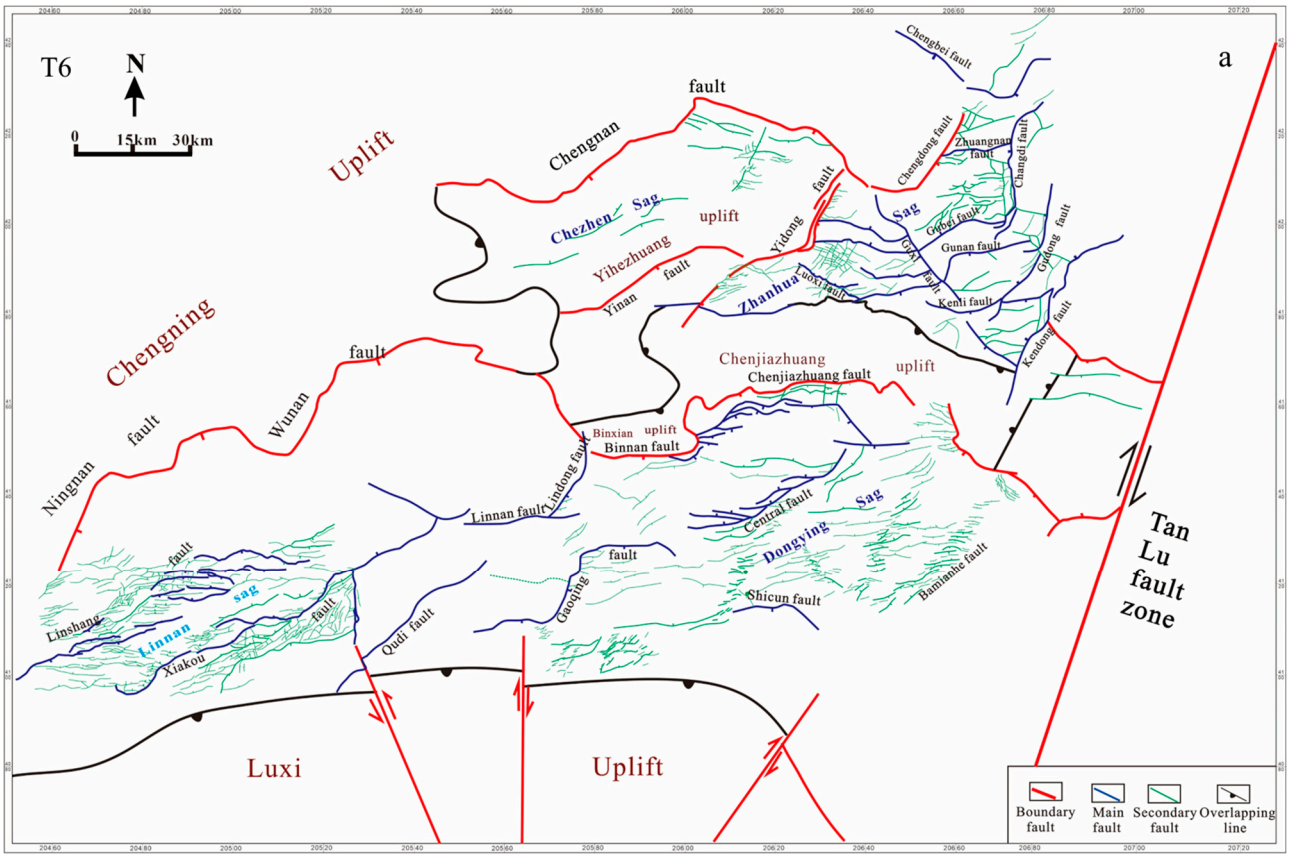

Figure 10. *Cont.*

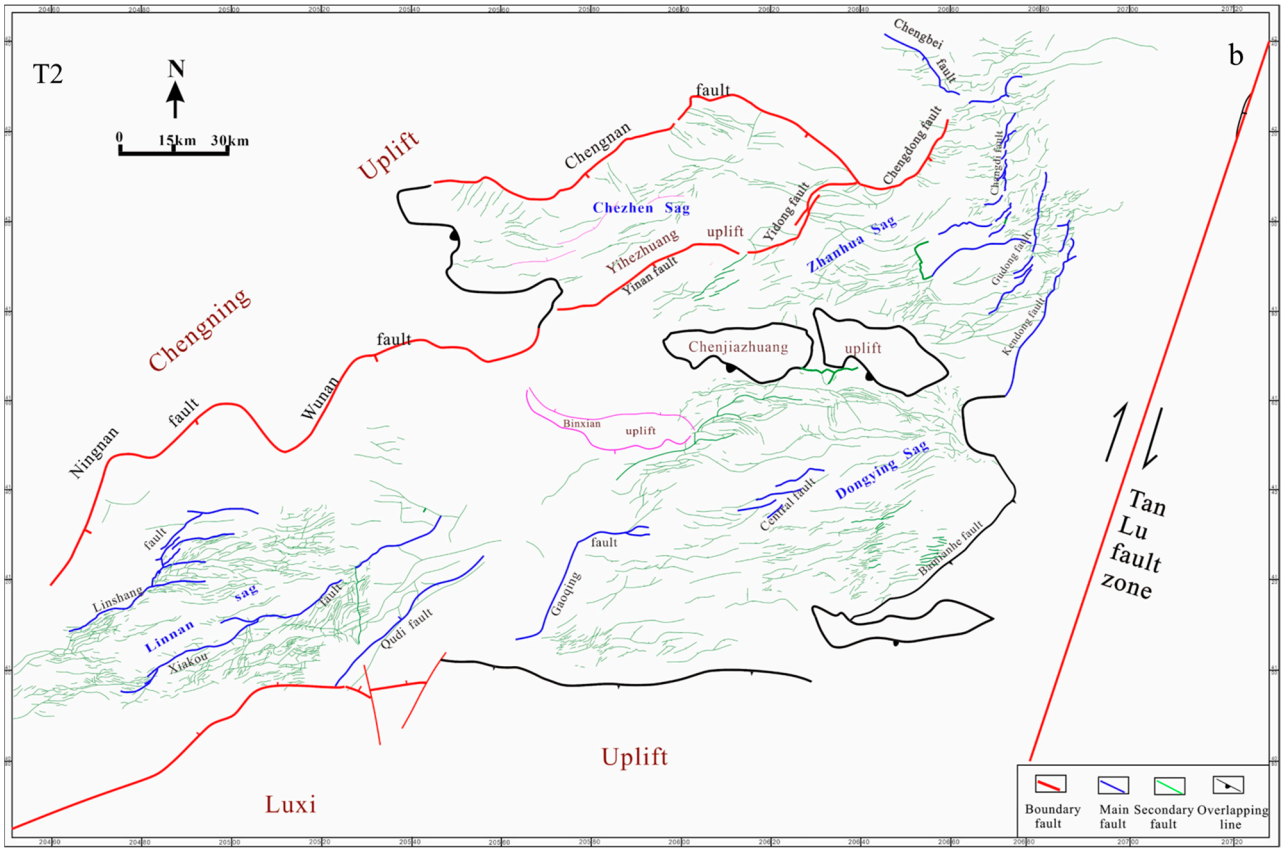

Figure 10. Fault system map of different formations in the Jiyang Depression. (**a**) Fault system map of the Es_3 member in the Jiyang Depression. The NNE- and NW-striking faults continue in the eastern part of the study area. NE-striking faults continue in the western of the study area. (**b**) Fault system map of the Ed formation in the Jiyang Depression. The NW-striking faults disappeared. The NE- and ENE-striking faults developed in this stage.

We have shown that the fault pattern at the base of the syn-rift section in the Jiyang Depression is dominated by NW- and NE-striking boundary faults (Late Mesozoic to Paleocene) [8,46]. Then, in the early Eocene, NE-striking and NNE-striking faults developed within the depression. Most of the NE- and NNE-striking faults cut downwards through the Cenozoic strata. The origin of the NE-striking faults was due to the NNW-oriented extensional stress and developed in the whole study area. The origin of the NNE-striking faults was due to the oblique extensional reactivation of the pre-existing NW-striking faults and the NNE-striking faults are best developed on the eastern side and show an en-echelon pattern (Figure 10a). Until the Middle Eocene, the ENE-striking faults were activated and developed in the tips of the NE- and NNE-striking faults and formed horsetail patterns. The new faults (EW-striking faults) were able to develop with thicker sediments and a more stable basement, as well as in areas with a lower density of pre-existing faults (Figure 10b).

6. Discussion

6.1. Analysis of Control Factors for the Development of Fault Patterns in the Jiyang Depression

Previously, we discussed how the combination of existing faults and various stress phases impacted the modifications in fault patterns within the Jiyang Depression. On a larger scale, the BBB experienced a collision between the South China continent and the North China Craton during the Late Triassic, resulting in land–land convergence. This convergence process generated thrust faults oriented towards the north in multiple regions within the BBB. As time progressed into the Early Cretaceous epoch, the region underwent extensional rifting, causing the previously existing NW-striking thrust faults to transform

into normal faults. During the Cenozoic era, the BBB resided in the subduction zone between the Pacific plate and the Eurasian plate. Between 66 and 50 Ma, the subduction rate varied from 120–140 mm/year around 80 Ma to 80–100 mm/year approximately 60 Ma [8,37,47]. During the Cenozoic era, the BBB resided in the subduction zone between the Pacific plate and the Eurasian plate [48,49]. The steep subduction resulted in mantle upwelling, leading to NNW–SSE extension and the initiation of rift formation. Under regional oblique extension, the NW-striking faults were reactivated, while NE-striking faults developed within the basin. From 56 to 43 Ma, the Pacific plate continued its NNW movement [50,51], and the subduction rate decreased from 80 mm/year to 60 mm/year [48,49]. Most NW-striking faults in the basin ceased activity, with only a few remaining active (Chengbei Sag, Zhanhua Sag).

A number of NE-striking faults originated as a result of the interplay between pre-existing faults and the Tan–Lu strike-slip fault zone. These geological processes led to the formation of a succession of NNE-striking faults, exhibiting an en-echelon arrangement extending towards the NW orientation. Between 43 and 32 Ma, the Pacific plate transitioned from NNW to NWW-trending movement [50], and the subduction rate continued to decline. Consequently, the regional stress shifted to NS extension. During this period, newly formed EW-striking faults connected with NE-striking faults, giving rise to extensive ENE-striking faults that controlled the deposition within the basin [2,9]. The NNE-striking faults showcased strike-slip characteristics [20]. Starting from 23 Ma, the Pacific plate's subduction weakened, resulting in lower-intensity extension within the BBB. This initiated thermal subsidence in the BBB, causing primary fault activity to weaken or cease, leaving behind a series of secondary fractures in the shallow layer [52].

The influence of multi-phase extension on fault patterns has been demonstrated through analog models [24,53]. These experiments illustrate that faults created in the second phase are perpendicular to the direction of tension and intersect with or alter the orientation near the faults produced in the first phase. In recent years, seismic data from various regions, including the North Sea [14,54], Thailand Basin [17], and Bohai Bay Basin [20], have provided insights into natural fault patterns. Analysis of these examples reveals how pre-existing faults differentially impact the development of subsequent fault patterns. Similarly, the Jiyang Depression exhibits a diverse range of patterns: (1) In areas without pre-existing faults, NNW extension during the early Cenozoic led to the formation of numerous NE-striking faults. As the stress rotated clockwise from a NNW to NS extension, a significant number of EW-striking faults developed within the basin. These EW-striking faults interconnected with NE-striking faults, creating boundary faults for the sags in the basin. These faults exhibit a curved pattern, exemplified by faults like the Xiakou and Linshang faults [2,9] (Figure 11a). (2) In areas where pre-existing faults are present, during the early Cenozoic, a portion of the NW-striking faults became inactive and transformed into weak surfaces. This led to the formation of a series of NNE-striking faults, exhibiting an en-echelon style extending towards the NW orientation. When the second phase of extension occurred, the NNE-striking faults experienced stretching due to NS extension, exhibiting a strike-slip nature. The resulting EW-striking fault formed at their tips was influenced to bend in an ENE-striking manner. Together, they formed a horsetail structure that controlled the evolution of the eastern part of the Jiyang Depression (Figure 11b). (3) In areas where pre-existing faults were present, during the early Cenozoic, a portion of the NW-striking faults remained active. These active faults connected with the later-formed ENE-striking faults, controlling the structure of the basin (Figure 11c).

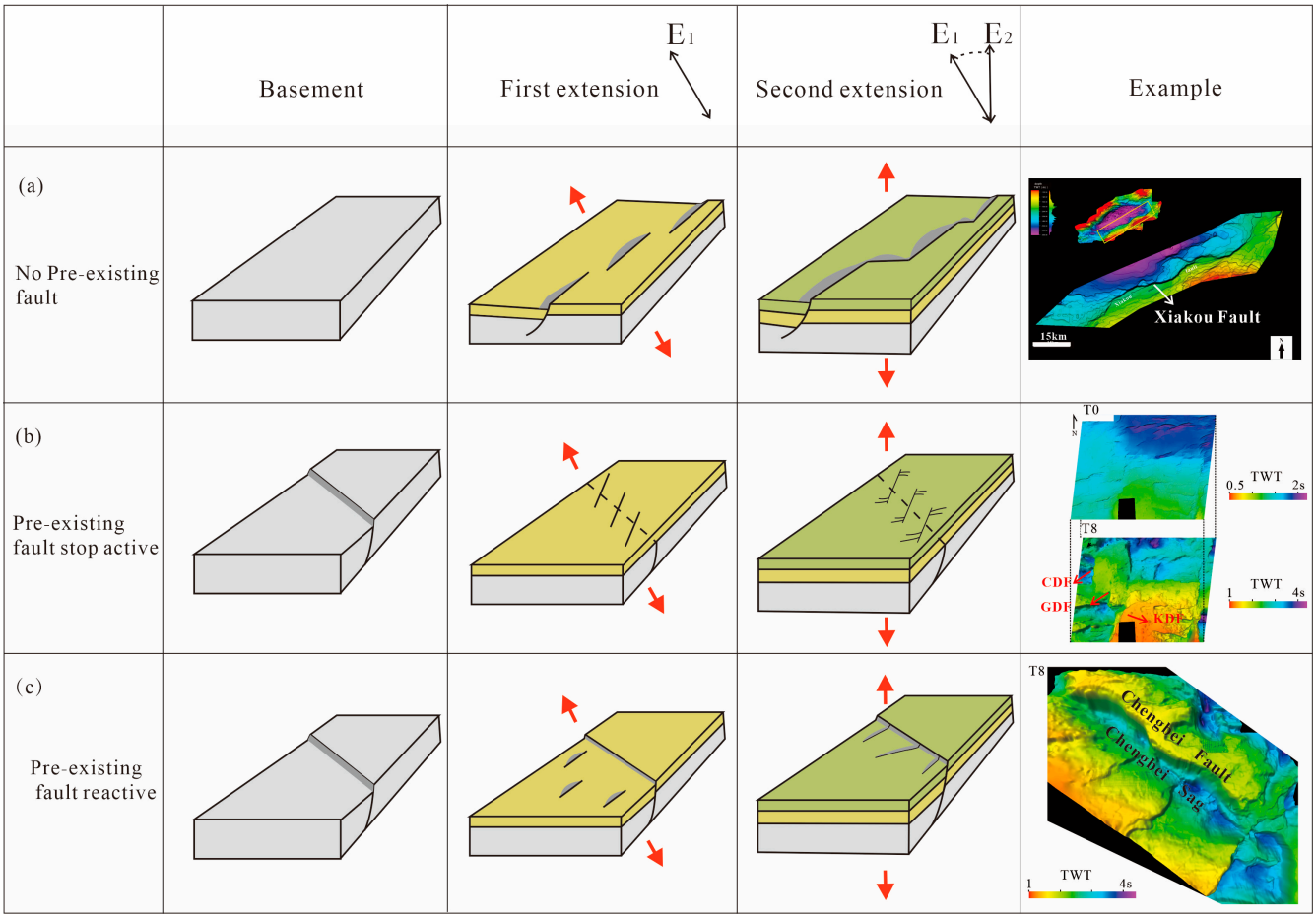

Figure 11. Simplified models showing the influence of multi-phase extension and pre-existing fault reactivation on the fault pattern. (**a**) During the first extension, areas without pre-existing faults formed NE-striking normal faults perpendicular to the extension direction. During the second extension, the newly formed EW-striking faults connected with the early NE-striking faults, forming a large ENE-striking fault that exhibited "zigzag" characteristics. (**b**) During the first extension, the pre-existing fault stopped being active. The NNE-striking fault were active and exhibited an en-echelon arrangement extending towards the NW orientation. During the second extension, NNE-striking faults and newly generated ENE-striking faults formed horsetail structures. (**c**) During the first extension, the pre-existing fault reactivated under oblique extension, and the NE-striking fault approached the pre-existing fault. During the second extension, the newly formed faults intersected the pre-existing fault, leading to the basin structure complex. Abbreviations: CDF, Changdi Fault; GDF, Gudong Fault; KDF, Kendong Fault.

6.2. Implications for Hydrocarbon Exploration by Multi-Phase Extension

During previous exploration efforts, numerous reservoirs within the Jiyang Depression were found to be abundant in hydrocarbon resources. The source rocks of the Jiyang Depression are manly located in the Eocene period, and Shahejie-3 Formation (early Eocene) is the main source rock layer. There are two hydrocarbon expulsion periods, Dongying Formation (Oligocene) and Guantao Formation (Miocene), and the Guantao Formation is the main hydrocarbon expulsion period. In the research area, certain reservoirs contained only water and lacked any hydrocarbon resources. This discrepancy can likely be attributed to the disruption of reservoirs and the diffusion of hydrocarbons caused by multi-phase extension and pre-existing fault activity. The fault system resulting from the combination of multi-phase extension and pre-existing faults had various effects on the transport and accumulation of hydrocarbons [9,33,55]: (1) Pre-existing and boundary faults that formed early cut through reservoirs and source rocks, serving as excellent conduits for vertical

hydrocarbon transport. For example, the Chengbei Sag is located in the southeast part of the research area. The Chengbei Fault boundary, as a pre-existing fault, was later subjected to multiphase extension and reactivation (Figures 6 and 10), accumulating rich hydrocarbon reservoirs in different layers. (2) Late-developed EW-striking faults and early-developed NE-striking faults connected with each other to create curved faults. In areas where the strike changes occurred, hard linkages formed a transfer zone. These zones often act as conduits for material sources to enter the basin, making them highly favorable for hydrocarbon accumulation. For example, the Xiakou Fault and Linshang Fault in the southwest part of the research area are combinations of this fault pattern (Figures 4c and 10). After a long period of exploration, a large number of oil reservoirs have been discovered in their hanging walls. (3) Faults striking in the EW and NS directions, developed within the rock layers, can increase the number of traps and expand their area. Although these faults are relatively smaller in size, less displaced, less active, and consistently closed, they tend to become reservoirs more easily for hydrocarbon storage. These small faults have been discovered in the Linnan Sag in the southwest part of the study area and the Tanhai area in the east part of the study area (Figures 8 and 10), which have good sealing properties and are favorable hydrocarbon reservoirs. When conducting hydrocarbon exploration, it is preferable to focus on the first and second types of faults during the early stages. These types have the potential to lead to the discovery of additional hydrocarbon reservoirs. Conversely, mature basins that have already reached a high water-bearing stage should prioritize exploration of the third type of fault.

7. Conclusions

This study discusses the fault pattern evolution in rift basins under multi-phase extension. We show that pre-existing faults subjected to multi-phase extension exhibit different reactivation characteristics, affecting later fault patterns. The Jiyang Depression is a “natural laboratory” in which we can study the influence of multi-phase extension on fault pattern evolution.

We found five fault patterns in the study area: Type 1 NW-striking pre-existing faults, Type 2 newly formed NNE-striking faults intersecting the extension direction at a small angle, Type 3 newly formed NE-striking faults that are linked by NE- and EW-striking faults, Type 4 newly formed ENE-striking faults that are perpendicular to the extension direction, and Type 5 newly formed NS-striking faults, which developed on a small scale and mainly occur in the fault blocks. The fault pattern evolution is affected by stress changes and the pre-existing faults were reactivated at a later stage.

Stress changes significantly affect the evolution of fault patterns. Pre-existing faults undergo reactivation during later stages. All fault patterns observed in the Jiyang Depression experienced distinct evolutions. Pre-existing faults undergo extension and reactivation, while new faults develop in shallow layers following an en-echelon pattern. Curved faults in the study area formed later than pre-existing faults due to clockwise regional stress changes in the Cenozoic era. Faults with different orientations, which formed during various periods, eventually became hard-linked and take on a zig-zag pattern as curved faults.

The combination of multi-phase extension and pre-existing faults leads to diverse fault patterns with varied roles during different stages of hydrocarbon exploration. Type 1, type 2, and type 3 faults are particularly suitable for early-stage exploration, often resulting in the discovery of larger hydrocarbon reservoirs. In contrast, type 4 and type 5 faults are more appropriate for mature exploration areas, where they may reveal smaller hydrocarbon reservoirs.

In this study, the reactivation of pre-existing faults is a key issue that involves many factors. In addition to the stress direction, fluids play an important role. Therefore, future studies of the impact of fluids on the activation of faults may be very challenging.

Author Contributions: Conceptualization, D.W.; methodology, W.L.; software, D.W., L.Y. and X.W.; validation, X.W.; investigation, L.Y.; resources, L.Y. and W.L.; data curation, L.Y., W.L. and X.W.; writing—original draft preparation, D.W.; writing—review and editing, L.Y.; supervision, D.W.;

project administration, D.W.; funding acquisition, D.W. All authors have read and agreed to the published version of the manuscript.

Funding: This research was funded by the National Nature Science Foundation of China (Project number 42072169), the Natural Science Foundation of Xinjiang Uygur Autonomous Region (Project number 2022D01C659), and the "Tianchi Talent" funded by Xinjiang Uygur Autonomous Region Introduction Plan.

Institutional Review Board Statement: Not applicable.

Informed Consent Statement: Not applicable.

Data Availability Statement: The data supporting the research results can be obtained from the China Petrochemical Corporation Shengli Oil Field, but the availability of these data is limited. These data are used under the permission for the current research, so they are not disclosed.

Acknowledgments: We thank the Shengli Oil Field Company, SINOPEC, and the individuals who contributed to the seismic data for this work.

Conflicts of Interest: The authors declare no conflict of interest.

References

1. Morley, C. Variations in late Cenozoic-recent strike-slip and oblique-extensional geometries, within Indochina: The influence of pre-existing fabrics. *J. Struct. Geol.* **2007**, *29*, 36–58. [CrossRef]
2. Wang, D.; Wu, Z.P.; Yang, L.L.; Liu, H.; Zhang, Y. Growth and linkage of the Xiakou fault in the Linnan Sag, Jiyang Depression, Eastern China: Formation mechanism and sedimentation response. *Mar. Petrol. Geol.* **2020**, *116*, 104319. [CrossRef]
3. Duffy, O.B.; Bell, R.B.; Jackson, C.A.L.; Gawthorpe, R.L.; Whipp, P.S. Fault growth and interactions in a multiphase rift fault network: Horda Platform, Norwegian North Sea. *J. Struct. Geol.* **2015**, *80*, 99–119. [CrossRef]
4. Fossen, H.; Rotevatn, A. Fault linkage and relay structures in extensional settings—A review. *Earth Sci. Rev.* **2016**, *154*, 14–28. [CrossRef]
5. Deng, H.D.; McClay, K.; Bilal, A. 3D structure and evolution of an extensional fault network of the eastern Dampier Sub-basin, North West Shelf of Australia. *J. Struct. Geol.* **2020**, *132*, 103972. [CrossRef]
6. Peacock, D.C.P.; Sanderson, D.J. Structural analyses and fracture network characterization: Seven pillars of wisdom. *Earth Sci. Rev.* **2018**, *184*, 13–28. [CrossRef]
7. Wu, Z.P.; Li, W.; Ren, Y.J.; Lin, C.S. Basin Evolution in the Mesozoic and Super Position of Cenozoic Basin in the Area of the Jiyang Depression. *Acta Geol. Sinica* **2003**, *77*, 280–286.
8. Ren, J.Y.; Yu, J.G.; Zhang, J.X. Structures of deep bed in Jiyang Sag and their control over the development of Mesozoic and Cenozoic basins. *Earth Sci. Front.* **2009**, *16*, 117–137.
9. Wang, D.; Wu, Z.P.; Yang, L.L.; Li, W.; He, C. Influence of two-phase extension on the fault network and its impact on hydrocarbon migration in the Linnan sag, Bohai Bay Basin, East China. *J. Struct. Geol.* **2021**, *145*, 104289. [CrossRef]
10. Chen, N.; Li, C.F.; Wen, Y.L.; Wang, P.; Zhao, X.L.; Wan, X.L. Seismic Multiple Attenuation in the Continent–Ocean Transition Zone of the Northern South China Sea. *J. Mar. Sci. Eng.* **2023**, *11*, 227. [CrossRef]
11. Yang, L.L.; Ren, J.Y.; Mclntosh, K.P.; Xiong, C.; Lei, C.; Zhao, Y.H. The structure and evolution of deepwater basins in the distal margin of the northern South China Sea and their implications for the formation of the continental margin. *Mar. Petrol. Geol.* **2018**, *92*, 234–254. [CrossRef]
12. Ye, Q.; Mei, L.F.; Shi, H.S.; Du, J.Y.; Deng, P.; Shu, Y.; Camanni, G. The Influence of Pre-existing Basement Faults on the Cenozoic Structure and Evolution of the Proximal Domain, Northern South China Sea Rifted Margin. *Tectonics* **2020**, *39*, e2019TC005845. [CrossRef]
13. Fossen, H. *Structural Geology*; Cambridge University Press: Cambridge, UK, 2010; pp. 361–366.
14. Deng, C.; Fossen, H.; Gawthorpe, R.; Rotevatn, A.; Jackson, C.A.L.; FazliKhani, H. Influence of fault reactivation during multiphase rifting: The Oseberg area, northern North Sea rift. *Mar. Petrol. Geol.* **2017**, *86*, 1252–1272. [CrossRef]
15. Phillips, T.B.; Fazlikhani, H.; Gawthorpe, R.; Fossen, H.; Jackson, C.A.L.; Bell, R.E.; Faleide, J.I.; Rotevatn, A. The influence of structural inheritance and multiphase extension on rift development, the NorthernNorth Sea. *Tectonics* **2019**, *38*, 4099–4126. [CrossRef]
16. Morley, C. The impact of multiple extension events, stress rotation and inherited fabrics on normal fault geometries and evolution in the Cenozoic rift basins of Thailand. *J. Geol. Soc. London* **2017**, *439*, 413. [CrossRef]
17. Pongwapee, S.; Morley, C.; Wonin, K. Impact of pre-existing fabrics and multi-phase oblique extension on Cenozoic fault patterns, Wichianburi sub-basin of the Phetchabun rift, Thailand. *J. Struct. Geol.* **2019**, *118*, 340–361. [CrossRef]
18. Gibson, G.M.; Totterdell, J.M.; White, L.T.; Mitchell, C.H.; Whitaker, A. Pre-existing basement structure and its influence on continental rifting and fracture zone development along Australia's southern rifted margin. *J. Geol. Soc. London* **2013**, *170*, 365–377. [CrossRef]

19. Deng, H.D.; McClay, K. Three-dimensional geometry and growth of a basement-involved fault network developed during multiphase extension, Enderby Terrace, NW Shelf of Australia. *GSA Bull.* **2021**, *133*, 2051–2078. [CrossRef]
20. Wang, D.; Zhang, X.Q.; Yang, L.L.; Chen, X.P.; Ma, S.T.; Wu, Z.P. Influence of pre-existing faults on Cenozoic structures in the Chengbei sag and Wuhaozhuang area, Bohai Bay Basin, East China. *Mar. Petrol. Geol.* **2022**, *138*, 105539. [CrossRef]
21. Whipp, P.; Jackson, C.A.L.; Gawthorpe, R.; Dreyer, T.; Quinn, D. Normal fault array evolution above a reactivated rift fabric; a subsurface example from the northern Horda Platform, Norwegian North Sea. *Basin Res.* **2014**, *26*, 523–549. [CrossRef]
22. Peacock, D.C.P.; Nixon, C.W.; Rotevatn, A.; Sanderson, D.J.; Zuluaga, L.F. Interacting faults. *J. Struct. Geol.* **2017**, *97*, 1–22. [CrossRef]
23. Nixon, C.W.; Sanderson, D.J.; Dee, S.J.; Bull, J.M.; Humphreys, R.J.; Swanson, M.H. Fault interactions and reactivation within a normal fault network at Milne Point, Alaska. *AAPG Bull.* **2014**, *98*, 2081–2107. [CrossRef]
24. Withjack, M.O.; Henza, A.A.; Schlische, R. Three-dimensional fault geometries and interactions within experimental models of multiphase extension. *AAPG Bull.* **2017**, *101*, 1767–1789. [CrossRef]
25. Peacock, D.C.P.; Sanderson, D.J.; Rotevatn, A. Reationship between fractures. *J. Struct. Geol.* **2018**, *106*, 41–53. [CrossRef]
26. Peacock, D.C.P.; Nixon, C.W.; Rotevatn, A.; Sanderson, D.J.; Zuluaga, L.F. Glossary of fault and other fracture networks. *J. Struct. Geol.* **2016**, *92*, 12–29. [CrossRef]
27. Wu, D.; Zhu, X.M.; Su, Y.D.; Li, Y.T.; Li, Z.; Zhou, Y.Y.; Zhang, M.Y. Tectono-sequence stratigraphic analysis of the Lower Cretaceous Abu Gabra Formation in the Fula Sub-basin, Muglad Basin, southern Sudan. *Mar. Petrol. Geol.* **2015**, *67*, 286–306. [CrossRef]
28. Henstra, G.A.; Gawthorpe, R.L.; Helland-Hansen, W.; Ravnas, R.; Rotevatn, A. Depositional systems in multiphase rifts: Seismic case study from the Lofoten margin, Norway. *Basin Res.* **2016**, *47*, 447–469. [CrossRef]
29. Huang, L.; Liu, C.Y.; Kusky, T.M. Cenozoic evolution of the Tan-Lu Fault Zone (East China)-Constraints from seismic data. *Gondwana Res.* **2015**, *28*, 1079–1095. [CrossRef]
30. Ren, J.Y.; Tamaki, K.; Li, S.T.; Zhang, J.X. Late Mesozoic and Cenozoic rifting and its dynamic setting in Eastern China and adjacent areas. *Tectonophysics* **2002**, *344*, 175–205. [CrossRef]
31. Huang, L.; Liu, C.Y. Three types of flower structures in a divergent-wrench fault zone. *J. Geophys. Res.-Solid Earth* **2017**, *122*, 10478–10497. [CrossRef]
32. Chen, X.P.; Li, W.; Wu, Z.P.; Yang, H.F.; Zhang, Q.; Meng, M.F.; Wang, G.Z.; Jia, H.B. The tectonic transition from rifting to strike-slip in the Liaodong Bay Depression, offshore China. *Mar. Petrol. Geol.* **2022**, *139*, 105598. [CrossRef]
33. Zhang, X.Q.; Zhang, G.C.; Jiang, Y.M.; Cui, M.; He, X.J. The control of curved faults on structural trap formation: Tiantai slope belt, Xihu Sag, East China Sea. *Mar. Petrol. Geol.* **2023**, *156*, 106464. [CrossRef]
34. Li, W.; Meng, M.F.; Zhang, T.J.; Chen, X.P.; Liu, Y.M.; Wang, D.; Yang, H.F.; Niu, C.M. New insights into the distribution and evolution of the WNW-directed faults in the Liaodong Bay sub-basin of Bohai Bay Basin, eastern China. *Front. Earth Sci.* **2022**, *9*, 763050. [CrossRef]
35. Qi, J.F.; Yang, Q. Cenozoic structural deformation and dynamic processes of the Bohai Bay basin province, China. *Mar. Pet. Geol.* **2010**, *27*, 757–771. [CrossRef]
36. Wang, G.Z.; Li, S.Z.; Suo, Y.H.; Zhang, X.Q.; Zhang, Z.; Wang, D.Y.; Liu, Z.; Liu, Y.M.; Zhou, J.; Wang, P.C.; et al. Deep-shallow coupling response of the Cenozoic Bohai Bay Basin to plate interactions around the Eurasian Plate. *Gondwana Res.* **2022**, *102*, 180–199. [CrossRef]
37. Liu, S.F.; Su, S.; Zhang, G.W. Early Mesozoic basin development in North China: Indications of cratonic deformation. *J. Asian Earth Sci.* **2013**, *62*, 221–236. [CrossRef]
38. Meng, Q.; Wu, G.; Fan, L.; Wei, H. Tectonic evolution of early Mesozoic sedimentary basins in the North China block. *Earth Sci. Rev.* **2019**, *190*, 416–438. [CrossRef]
39. Wang, Y.; Zhou, L.; Zhao, L. Cratonic reactivation and orogeny: An example from the northern margin of the North China Craton. *Gondwana Res.* **2013**, *24*, 1203–1222. [CrossRef]
40. Zhao, F.; Jiang, S.; Li, S.; Zhang, H.; Wang, G.; Lei, J.; Gao, S. Cenozoic tectonic migration in the Bohai Bay Basin, East China. *Geol. J.* **2016**, *51*, 188–202. [CrossRef]
41. Cheng, Y.J.; Wu, Z.P.; Lu, S.N.; Li, X.; Lin, C.Y.; Huang, Z.; Su, W.; Jiang, C.; Wang, S.Y. Mesozoic to Cenozoic tectonic transition process in Zhanhua Sag, Bohai Bay Basin, East China. *Tectonophysics* **2018**, *730*, 11–28. [CrossRef]
42. Li, Z.H.; Qu, H.J.; Gong, W.B. Late Mesozoic basin development and tectonic setting of the northern North China Craton. *J. Asian Earth Sci.* **2015**, *114*, 115–139. [CrossRef]
43. Liu, S.; Gurnis, M.; Ma, P.; Zhang, B. Reconstruction of northeast Asian deformation integrated with western Pacific plate subduction since 200 Ma. *Earth Sci. Rev.* **2017**, *175*, 114–142. [CrossRef]
44. Wu, Z.P.; Hou, X.B.; Li, W. Discussion on mesozoic basin patterns and evolution in the eastern North China block. *Geotect. Metallogenia.* **2007**, *31*, 385–399.
45. Zhu, G.; Wang, Y.S.; Liu, G.S.; Niu, M.L.; Xie, C.L.; Li, C.C. 40Ar/39Ar dating of strike-slip motion on the Tan–Lu fault zone, East China. *J. Struct. Geol.* **2005**, *27*, 1379–1398. [CrossRef]
46. Zheng, D.S.; Wu, Z.P.; Li, L.; Chen, Y.Z.; Li, W.; Zhou, Y.Q. Development characteristic of faults in Mesozoic and Cenozoic of Huimin Sag and its control to sediment. *J. Univ. Pet. China* **2004**, *28*, 6–12.

47. Zhang, F.P.; Wu, Z.P.; Li, W.; Zhu, J.C.; Fu, L.X.; Li, H.J.; Lou, D.; Zhao, Y.G. Structural characteristics and its tectonic evolution of Huanghua depression during the Indosinian-Yanshanian. *J. China Inst. Min. Technol.* **2019**, *48*, 792–807.
48. Maruyama, S.; Send, T. Orogeny and relative plate motions: Example of the Japanese Islands. *Tectonophysics* **1986**, *127*, 305–329. [CrossRef]
49. Northrup, C.J.; Royden, L.H.; Burchfiel, B.C. Motion of the Pacific plat e relative to Eurasia and its potential relation to Cenozoic extension along the eastern margin of Eurasia. *Geology* **1995**, *23*, 719–722. [CrossRef]
50. Müller, R.D.; Seton, M.; Zahirovic, S.; Williams, S.E.; Matthews, K.J.; Wright, N.M.; Shephard, G.E.; Maloney, K.T.; Barnett-Moore, N.; Hosseinpour, M.; et al. Ocean Basin evolution and global-scale plate reorganization events since Pangea breakup. *Annu. Rev. Earth Planet. Sci.* **2016**, *44*, 107–138. [CrossRef]
51. Zahirovic, S.; Seton, M.; Müller, R.D. The Cretaceous and Cenozoic tectonic evolution of Southeast Asia. *Solid Earth* **2014**, *5*, 227–273. [CrossRef]
52. Yu, Y.X.; Zhou, X.H.; Xu, C.G.; Wu, K.; Lv, D.Y.; Liu, Y.B.; Zhou, X. Architecture and evolution of the Cenozoic offshore Bohai Bay basin, eastern China. *J. Asian Earth Sci.* **2020**, *192*, 104272. [CrossRef]
53. Henza, A.A.; Withjack, M.O.; Schlische, R.W. Normal-fault development during two phases of non-coaxial extension: An experimental study. *J. Struct. Geol.* **2010**, *32*, 1656–1667. [CrossRef]
54. Henstra, G.A.; Berg, K.T.; Rotevatn, A.; Gawthorpe, R.L. How do pre-existing normal faults influence rift geometry? A comparison of adjacent basins with contrasting underlying structure on the Lofoten Margin, Norway. *Basin Res.* **2019**, *31*, 1083–1097. [CrossRef]
55. Fossen, H.; Schultz, R.A.; Rundhovde, E.; Rotevatn, A.; Buckley, S.J. Fault linkage and graben stepovers in the Canyonlands (Utah) and the North Sea Viking Graben, with implications for hydrocarbon migration and accumulation. *AAPG Bull.* **2010**, *94*, 597–613. [CrossRef]